miR-34a is upregulated in *AIP*-mutated somatotropinomas and promotes octreotide resistance

Eva-Maria Bogner, Adrian F. Daly, Sebastian Gulde, Auli Karhu, Martin Irmler, Johannes Beckers, Hermine Mohr, Albert Beckers, Natalia S. Pellegata.

Table of contents:

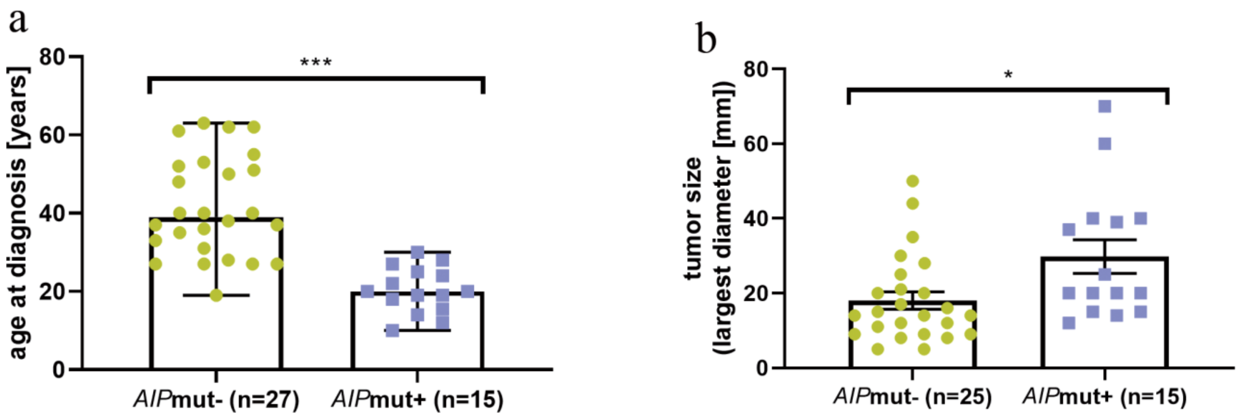

Supplementary Figure 1: Clinical parameters of the patient cohort. (a) age at diagnosis [years]. (b) largest tumor diameter [mm]. *, p>0,05; ***, p<0.001; (by unpaired t-test).

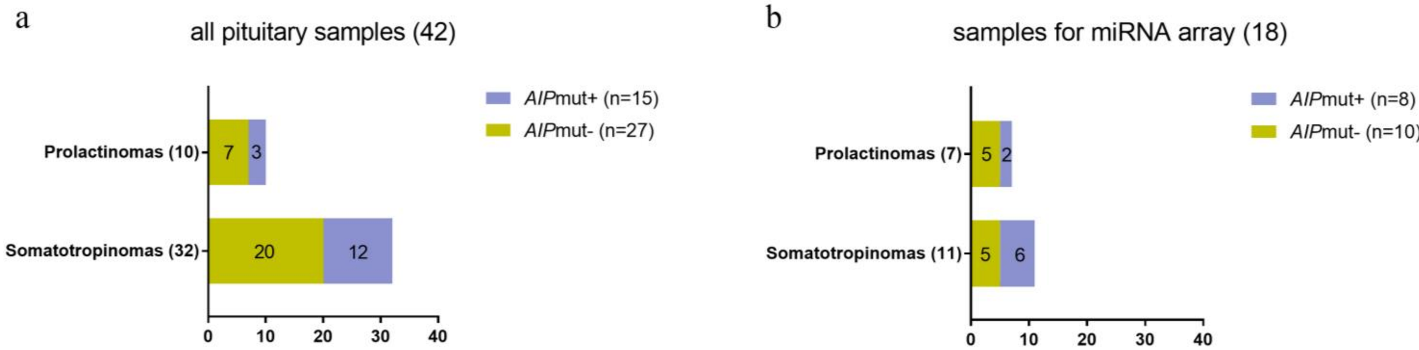

Supplementary Figure 2: Summary of primary pituitary adenoma samples used in the study. (a) A total of 42 PA samples was collected, including 27 AIPmut- tumors and 15 AIPmut+ pituitary adenomas. Samples comprised 10 prolactinomas (7 AIPmut-, 3 AIPmut+) and 32 somatotropinomas (20 AIPmut-, 12 AIPmut+), (b) Eighteen PAs were used for miRNA array analysis (7 prolactinomas: 5 AIPmut-, 2 AIPmut+; 11 somatotropinomas: 5 AIPmut-, 6 AIPmut+).

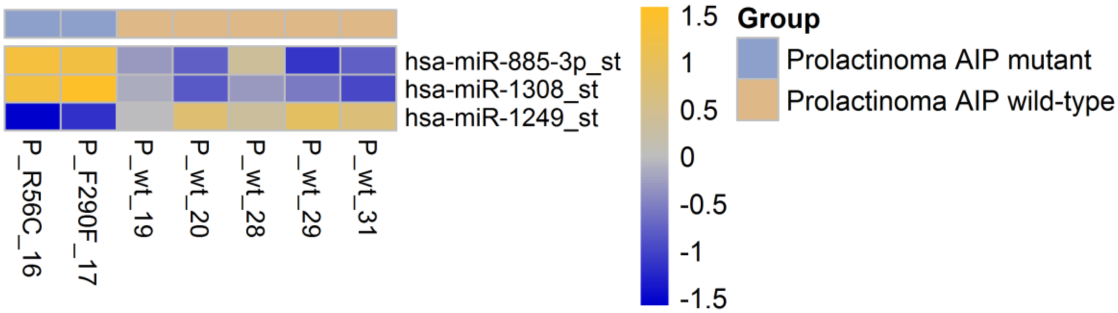

Supplementary Figure 3: Heat map of the most differentially expressed miRNAs ($p<0.002$, fold-change>1.5x) in prolactinomas (n=7). Yellow (blue) indicates higher (lower) expression level (z-scales to mean expression per row).

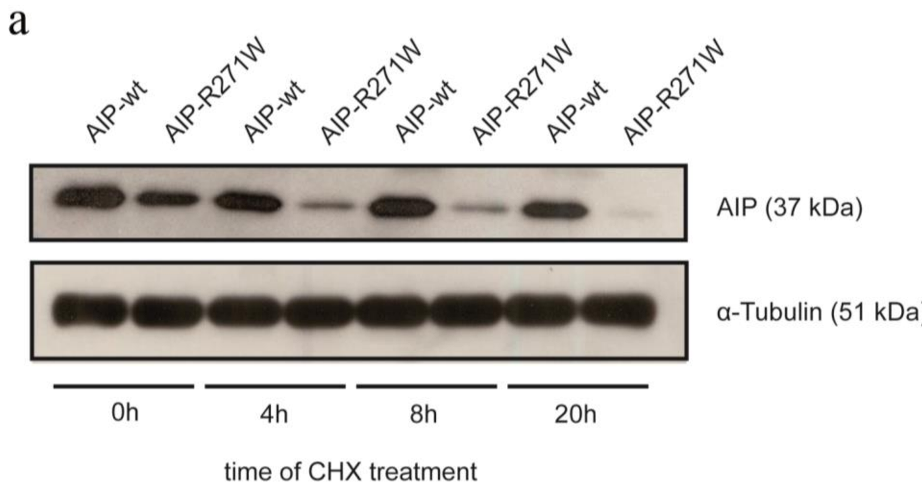

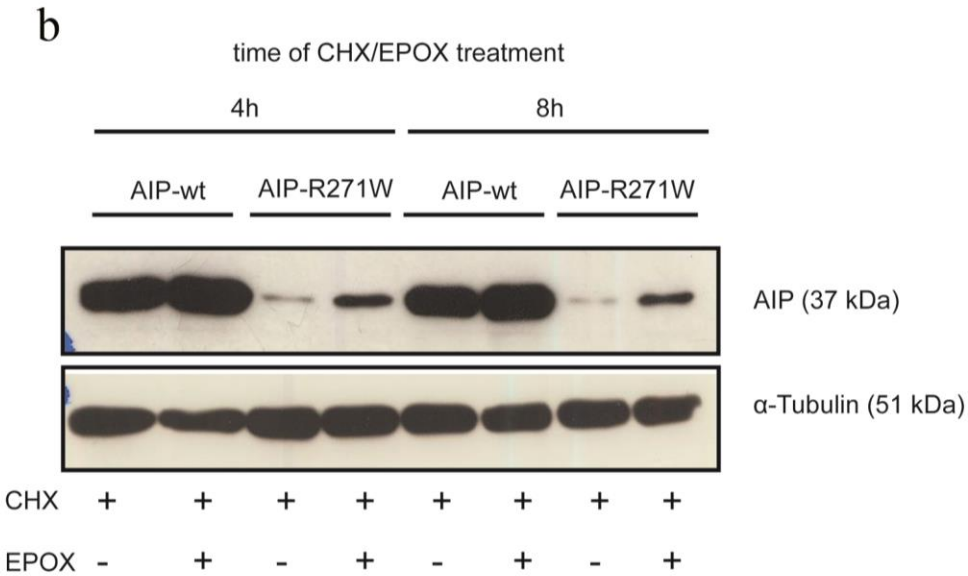

Supplementary Figure 4: AIP-R271W is less stable in vitro than AIP-wt. (a) Aip-/- MEFs transfected with AIP-wt or AIP-R271W constructs. Twenty-four h later cells were treated with 25µg/mL Cycloheximide (CHX) for the indicated times and collected for protein extraction. Western blot was performed using an anti-AIP antibody. α-Tubulin was used as loading control. (b) Aip-/- MEFs transfected as in (a) were treated with 25µg/mL CHX alone or in combination with 10µM Epoxomycin (EPOX) for the indicated times. Western blot was conducted as in (a).

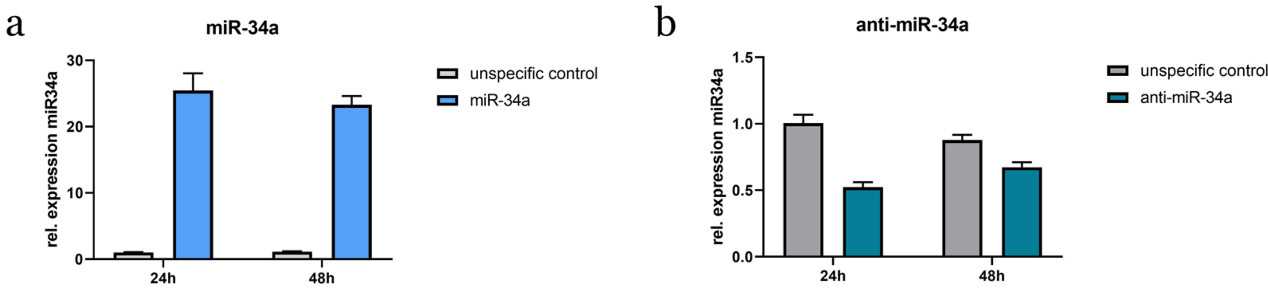

Supplementary Figure 5: miR-34a expression upon modulation with mimics and antagonists in GH3 and HEK293 cells. (a) GH3 cells were transfected with miR-34a mimics and the expression of the miRNA itself was assessed by qRT-PCR 24h and 48h post-transfection. (b) GH3 cells were transfected with anti-miR-34a and the expression of the miRNA itself was assessed as in a.

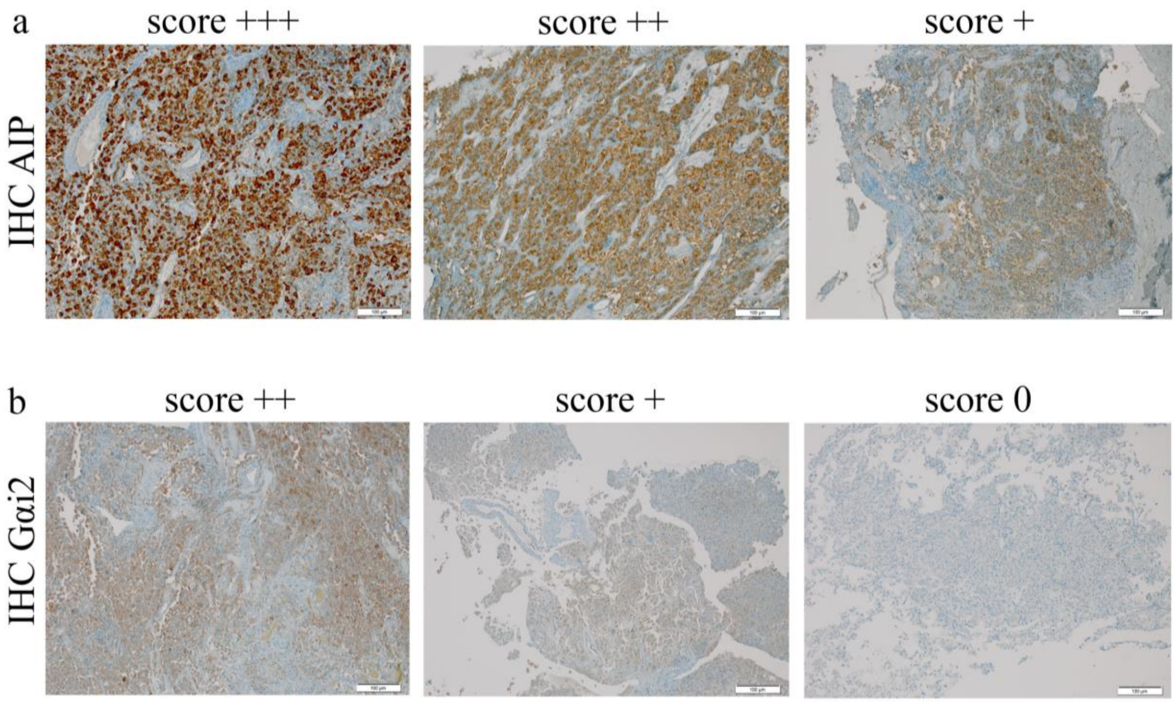

Supplementary Figure 6: PAs carrying the same AIP mutation (R271W) can display variable levels of (a) AIP and (b) Gαi2 expression. (a) AIP staining intensities of patient samples with the R271W variant have been scored with either +, ++ or +++. anti-AIP (1/1000) was used. Original magnification: x1000; scale bar = 100µm (b) Gαi2 staining intensities have been scored with either 0, + or ++. anti-Gαi2 (1/200) was used. Original magnification: x1000; scale bar = 100µm.

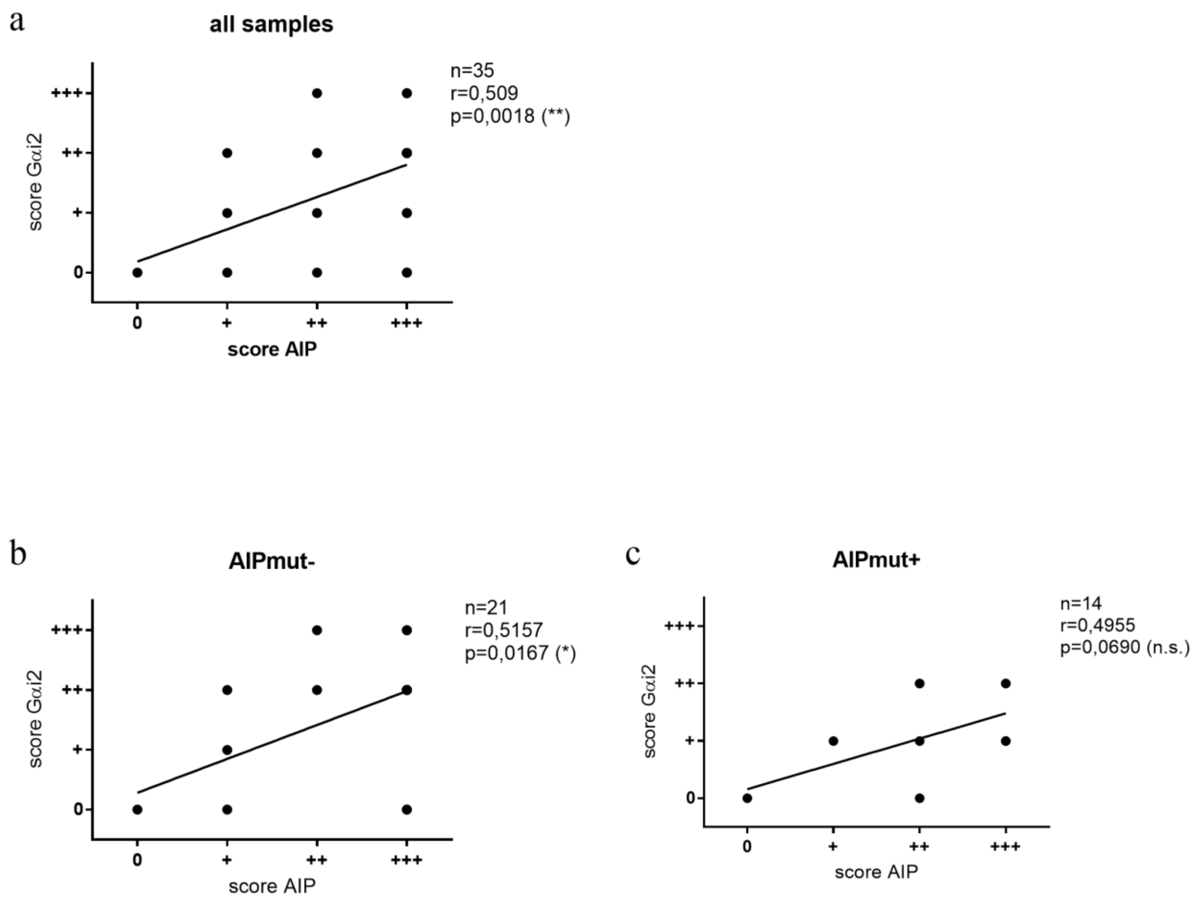

Supplementary Figure 7: Correlations of IHC scores of AIP and Gαi2. Correlations for (a) all samples (n=35), (b) AIPmut- PAs (somatotropinomas +prolactinomas; n=21), (c) AIPmut+ PAs (somatotropinomas +prolactinomas; n=14), Pearson correlation coefficients and two-tailed p value were computed. Linear regression was applied on the correlation. **, $p<0.01$; *, $p<0,05$; n.s., not significant.

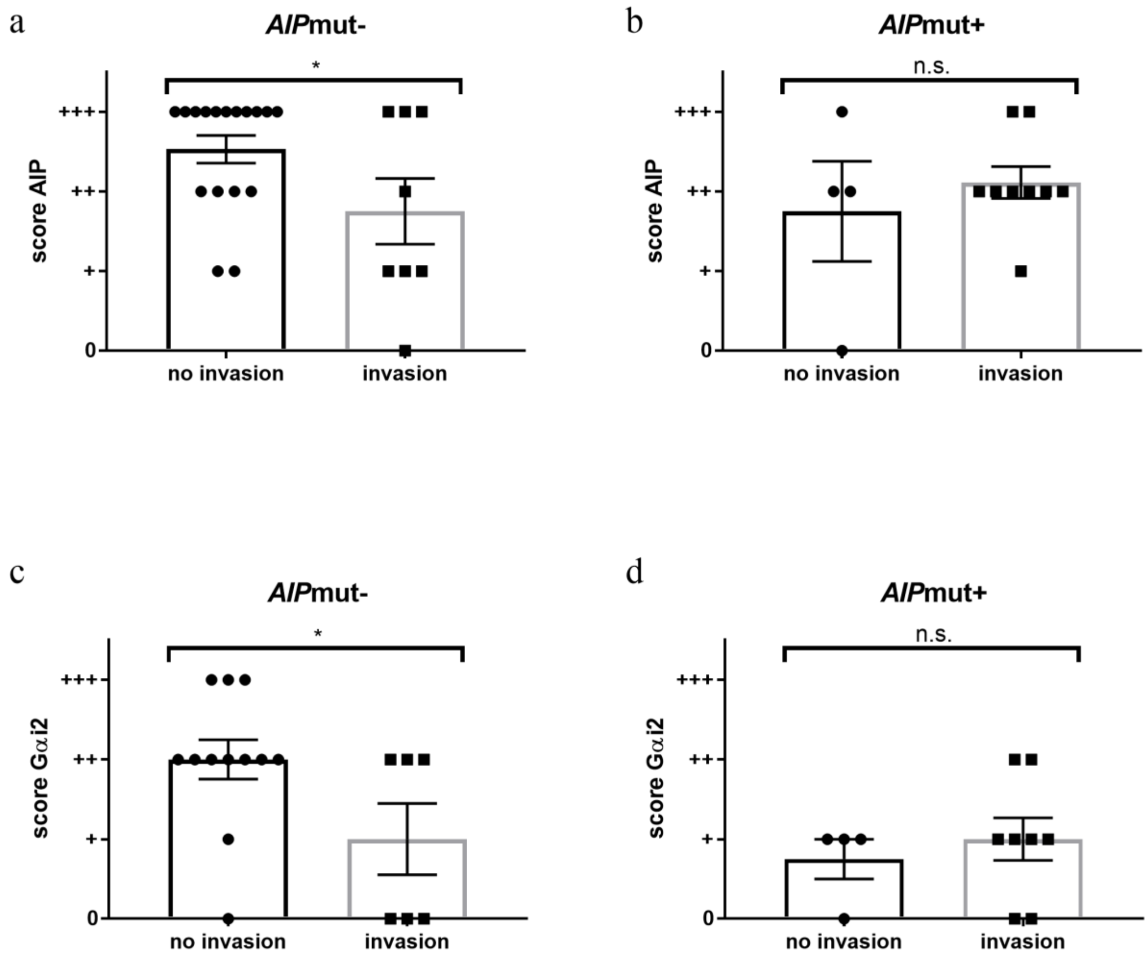

Supplementary Figure 8: Invasion occurs more often in patients with low Gαi2 expression. (a-b) AIP expression scores, (c-d) Gαi2 expression scores. AIPmut- (a, c) or AIPmut+ (b, d) were taken into the analysis. Results are reported as the mean ± SEM. **, p<0.01; ***, p<0,001 n.s., not significant; (by unpaired t-test).

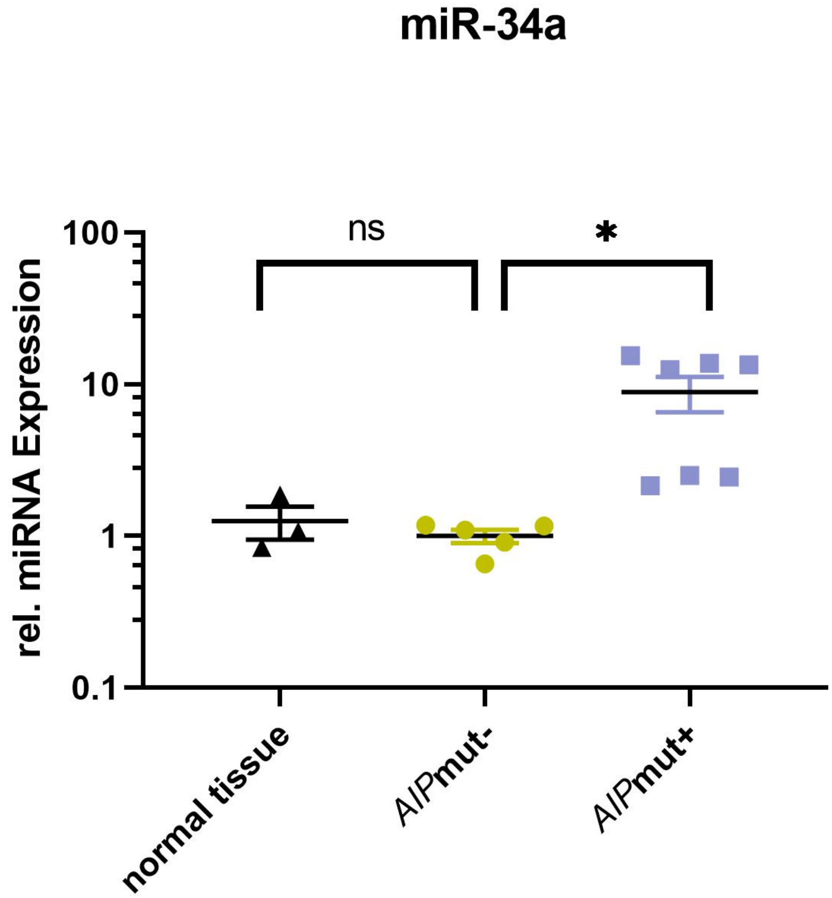

Supplementary Figure 9: Expression of miR-34a in normal human pituitary tissue. and in AIPmut- and AIPmut+ PAs.

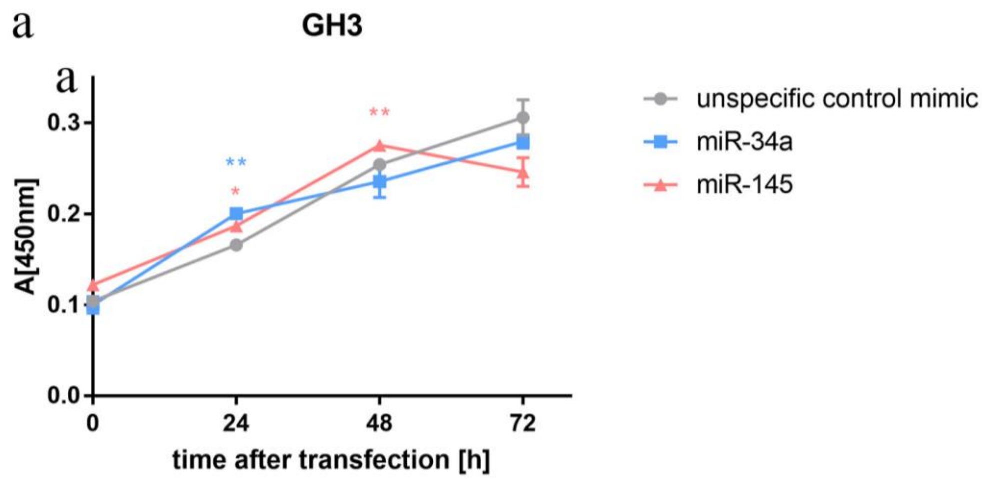

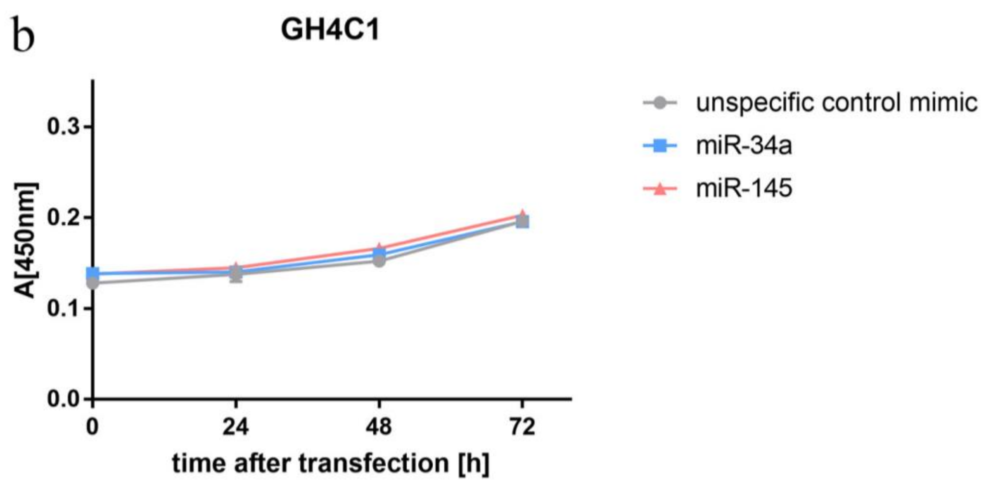

Supplementary Figure 10: Effect of miR34a and miR-145 on the proliferation of GH3 and GH4C1 cells. GH3 (a) and GH4C1 (b) cells were transfected with an unspecific miRNA mimic (unspecific control) or with specific mimics for mature miR-34a or miR-145. Cell viability was measured every day for up to 72h post-transfection. Only statistically significant changes are indicated. *, p>0,05; **, p>0,01 (by unpaired two-tailed Student's t-test.

Supplementary Table 1: List of patient samples with clinical parameters.

Patient ID	*AIP* Genotype	tumor type	sex	age at diagnosis	largest diameter, mm (classification)	Invasion	LOH *AIP*	score AIP	score Gαi2	Array ID (GH)	Array ID (PRL)
AIP1	wt	GH	f	36	14 (macro)	no		3			
AIP2	wt	GH	f	61	20 (macro)	yes		3	0		
AIP3	wt	GH	f	40	9 (micro)	no		3		S_wt_03	
AIP4	wt	GH	m	53	16 (macro)	no		3		S_wt_04	
AIP5	wt	GH	m	19	15 (macro)	yes		2	2		
AIP6	wt	GH	f	51	8 (micro)	no		3			
AIP7	wt	GH	f	52	14 (macro)	yes		3	2	S_wt_07	
AIP8	wt	GH	f	62	20 (macro)	yes		3		S_wt_08	
AIP9	wt	GH	m	33	30 (macro)	yes		1			
AIP10	wt	GH	m	48	12 (macro)	no		3	2		
AIP11	wt	GH	m	35	14 (macro)	no		3	3	S_wt_12	
AIP12	wt	GH	f	50	12 (macro)	no		3	2		
AIP13	R271W	GH	f	22	60 (macro)	yes	Yes	3	1	S_R271W_13 a/b	
AIP14	R271W	PRL	m	12	40 (macro)	no	Yes	2	1		excluded
AIP15	R271W	GH	m	15.5	15 (macro)	yes	Yes	2		S_R271W_15	
AIP16	R56C	PRL	m	25	70 (macro)	yes	Yes	2	1		P_R56C_16
AIP17	F269F	PRL	m	10	20 (macro)	yes	ND	2	0		P_F290F_17
AIP18	Q146S	GH	m	18	15 (macro)	yes	yes	2	0	S_Q146S_18	
AIP19	wt	PRL	m		50 (macro)	yes					P_wt_19
AIP20	wt	PRL	f	27	35 (macro)	yes					P_wt_20
AIP21	R271W	GH	m	20	20 (macro)	yes	yes	2	2	S_R271W_21	
AIP22	L115W	GH	f	19	37 (macro)	yes	yes			S_L115W_22	
AIP23	R128H	GH	m	28	20 (macro)	no	yes	2	1	S_R128H_24	
AIP24	M1I	GH	m	19	14 (macro)	no	yes	3	1		
AIP25	wt	PRL	f	63	44 (macro)	yes		0	0		P_wt_28
AIP26	wt	PRL	f	27	5 (micro)	no		1	1		P_wt_29
AIP27	wt	PRL	f	37	5 (micro)	no		1	0		
AIP28	wt	PRL	f	31	9 (micro)	no		2	2		P_wt_31
AIP29	wt	PRL	f	27	8 (micro)	yes		1	0		
AIP30	Q146S	GH	f	24	20 (macro)	yes	yes				
AIP31	R271W	GH	m	30	39 (macro)	yes	yes	1	1		
AIP32	R271W	GH	m	27	12 (macro)	no	ND	0	0		
AIP33	R271W	GH	m	20	25 (macro)	yes	yes	2	1		
AIP34	C238W	GH	m	14	40 (macro)	yes	yes	3	2		
AIP35	wt	GH	m	55	25 (macro)	yes		1	2		
AIP36	wt	GH	m	40	21 (macro)	no		3	2		
AIP37	wt	GH	f	62	9 (micro)	no		3	3		
AIP38	wt	GH	m	27	17 (macro)	no		3	2		
AIP39	wt	GH	f	38	11 (macro)	no		3	2		
AIP40	wt	GH	m	40	macro	no		2			
AIP41	wt	GH	f	37	micro	no		2	2		
AIP42	wt	GH	f	28	28 (macro)	no		2	3		

Supplementary Table 2: Primer and oligos for cloning and mutagenesis

Primer/Oligo name	sequence
AIP-EcoRI-Fw	GAGGCCCGAATTCGGATGGCGGATATCATCGCA
AIP-NotI-Rev	CCCCGCGGCCGCTCAATGGGAGAAGATCCCCCG
R271W-27nt-Fw	GGCCTACTTCAAGTGGGGCAAGGCCAA
R271W-27nt-Fw	TGGGCCTTGCCCCACTTGAAGTAGGCC
Oligo GNAI2 top	TCGAGATATAAGCTTTGTTCCAGACAACTGCCAATGTCACTGAGGGAAAGC
Oligo GNAI2 bottom	CTATATTCGAAACAAGGTCTGTTGACGGTTACAGTGACTCCCTTTCGCCGG
Oligo GNAI2 mut top	TCGAGATATAAGCTTTGTTCCCTGAGGGAAAGC
Oligo GNAI2 mut bottom	CTATATTCGAAACAAGGGACTCCCTTTCGCCGG

Supplementary Table 3: Primary antibodies used in the study. Abbreviations: WB: Western Blot, IHC: Immunhistochemistry

Target Protein	**Application**	**Dilution**	**Catalogue number**	**Company**
anti-AIP	WB IHC	1:750 1:1000	#NB100-127 #NB100-127	Novus Biologicals Inc., Littleton, CO, USA
anti-p44/42 MAPK (Erk1/2) (137F5)	WB	1:1000	#4695	Cell Signaling Technology, Danvers, MA, USA
anti-P-p44/42 MAPK (T202/Y204) (20G11)	WB	1:1000	#4376	Cell Signaling Technology, Danvers, MA, USA
anti-Gαi2	IHC	1:200	#ab157204	Abcam, Cambridge, UK
anti-α-tubulin	WB	1:1000	#T8203-200UL	Sigma-Aldrich, St. Louis, MO, USA

Supplementary Table 4: Cell lines and respective culture method. Abbreviations: FBS: fetal bovine serum, HS: horse serum; pen/strep: Penicillin-Streptomycin

Cell line	**Medium**	**Supplement**
GH3	F12K (#21127-022, Invitrogen, Carlsbad, CA, USA)	2.5 % FBS (#10500-064, Invitrogen, Carlsbad, CA, USA) 15 % HS (#26050088, Invitrogen, Carlsbad, CA, USA) 1 % pen/strep 5,000 U/ml (#15070063, Gibco/Invitrogen, Grand Island, NY, USA)
Mouse embryonic fibroblasts from AIP knockout mice (MEF AIP -/-)	DMEM + GlutaMAXTM-I, 4.5 g/l D-glucose, pyruvate (#11965-092, Gibco/Invitrogen, Grand Island, NY, USA)	15 % FBS 1 % pen/strep 1 % Fungizone™ (#15290026, Gibco/Invitrogen, Grand Island, NY, USA).
HEK293 cells	DMEM + GlutaMAXTM-I, 4.5 g/l D-glucose, pyruvate	15 % FBS and 1 % pen/strep
GH4C1	Ham's F10 (#11550043, Gibco/Invitrogen, Grand Island, NY, USA)	HS, 15%; FBS, 2.5%

Supplementary Table 5: miRNA mimics and inhibitors used in the study.

Name	Modulation	Species	Catalogue number	Company
miRIDIAN microRNA rno-miR-34a	Mimic	rat	#C-320335-05	Dharmacon, Inc., Lafayette, CO, USA
miRIDIAN microRNA Rat rno-miR-34a inhibitor	Inhibition	rat	#IH-320335-06	Dharmacon, Inc., Lafayette, CO, USA
anti-miR-34a	Inhibition	mouse	#IH-320335-06-0002	GE Healthcare, Little Chalfont, United Kingdom
miRIDIAN microRNA rno-miR-145 mimic	Mimic	rat	#C-320377-05	Dharmacon, Inc., Lafayette, CO, USA
anti-miR-145	Inhibition	mouse	#IH-320377-06-0002	GE Healthcare, Little Chalfont, United Kingdom
miRIDIAN microRNA Mimic Negative Control #1	negative control Mimic	human, mouse, rat	# CN-001000-01	Dharmacon, Inc., Lafayette, CO, USA
Hairpin Inhibitor Negative Control #1	negative control Inhibition	human, mouse, rat	#IN-001005-01-05	Dharmacon, Inc., Lafayette, CO, USA

Supplementary Table 6: List of target prediction algorithms and of the features they use for prediction (adapted from)

Prediction algorithm	Seed match	Conserva-tion	Free energy	Site accessibility	Target-site abundance	Machine learning	Online link
TargetScan 7.0	X	X					http://www.targetscan.org/vert_70/
miRANDA-mirSVR	X	X	X	X			http://www.microrna.org/microrna/home.do
DIANA tools	X	X	X	X	X	X	http://diana.imis.athena-innovation.gr/DianaTools/index.php
PITA	X	X	X	X	X		https://genie.weizmann.ac.il/pubs/mir07/mir07_prediction.html

Supplementary Table 7: Significantly enriched terms (p<0.01) associated with differentially expressed miRNAs between AIPmut+ and AIPmut- somatotropinomas. hsa-miR-497_st and hsa-miR-195_st are represented by miR-16-5p. Results with less than four miRNAs are not shown

Categories	Diseases or Functions Annotation	miRNAs	# miRNAs	p-value
Cancer, Connective Tissue Disorders, Organismal Injury and Abnormalities	Dedifferentiated liposarcoma	miR-143-3p, miR-145-5p, miR-16-5p, miR-26a-5p, miR-34a-5p	5	9.0E-13
Cancer, Organismal Injury and Abnormalities, Reproductive System Disease	Early stage invasive cervical squamous cell carcinoma	miR-145-5p, miR-16-5p, miR-187-3p, miR-26a-5p, miR-34a-5p	5	4.7E-12
Cell Cycle	Arrest in cell cycle progression	miR-145-5p, miR-16-5p, miR-26a-5p, miR-34a-5p	4	2.6E-06
Organismal Injury and Abnormalities, Reproductive System Disease	Endometriosis	miR-143-3p, miR-145-5p, miR-16-5p, miR-34a-5p	4	5.0E-06
Cellular Movement	Cell movement of tumor cell lines	miR-143-3p, miR-145-5p, miR-16-5p, miR-26a-5p, miR-34a-5p	5	7.3E-06
Metabolic Disease, Neurological Disease, Organismal Injury and Abnormalities, Psychological Disorders	Alzheimer disease	miR-145-5p, miR-16-5p, miR-26a-5p, miR-34a-5p	4	3.0E-05
Cellular Movement	Migration of tumor cell lines	miR-143-3p, miR-16-5p, miR-26a-5p, miR-34a-5p	4	1.2E-04
Cellular Development, Cellular Growth and Proliferation	Cell proliferation of tumor cell lines	miR-143-3p, miR-145-5p, miR-16-5p, miR-26a-5p, miR-34a-5p	5	1.2E-04
Cancer, Organismal Injury and Abnormalities	Squamous-cell carcinoma	miR-143-3p, miR-145-5p, miR-16-5p, miR-187-3p, miR-26a-5p, miR-34a-5p	6	1.2E-04
Cancer, Organismal Injury and Abnormalities	Upper aero-digestive squamous cell carcinoma	miR-143-3p, miR-145-5p, miR-16-5p, miR-26a-5p	4	1.4E-04
Inflammatory Response	Inflammation of body cavity	miR-143-3p, miR-145-5p, miR-16-5p, miR-26a-5p	4	1.5E-04
Inflammatory Response	Inflammation of absolute anatomical region	miR-143-3p, miR-145-5p, miR-16-5p, miR-26a-5p	4	3.5E-04
Cancer, Organismal Injury and Abnormalities, Respiratory Disease	Respiratory system tumor	miR-143-3p, miR-145-5p, miR-16-5p, miR-26a-5p, miR-34a-5p	5	6.9E-04
Cell Death and Survival	Apoptosis of tumor cell lines	miR-143-3p, miR-145-5p, miR-16-5p, miR-34a-5p	4	7.1E-04
Inflammatory Response, Organismal Injury and Abnormalities	Inflammation of organ	miR-143-3p, miR-145-5p, miR-16-5p, miR-26a-5p	4	9.3E-04
Cell Death and Survival	Apoptosis	miR-143-3p, miR-145-5p, miR-16-5p, miR-26a-5p, miR-34a-5p	5	1.1E-03
Cell Death and Survival	Cell viability	miR-143-3p, miR-145-5p, miR-16-5p, miR-34a-5p	4	1.2E-03
Cell Death and Survival	Necrosis	miR-143-3p, miR-145-5p, miR-16-5p, miR-26a-5p, miR-34a-5p	5	1.2E-03
Cancer, Organismal Injury and Abnormalities, Renal and Urological Disease	Urinary tract tumor	miR-143-3p, miR-145-5p, miR-16-5p, miR-26a-5p	4	1.3E-03

Cancer, Gastrointestinal Disease, Organismal Injury and Abnormalities	Upper gastrointestinal carcinoma	miR-143-3p, miR-145-5p, miR-16-5p, miR-26a-5p	4	5.1E-03
Cancer, Endocrine System Disorders, Gastrointestinal Disease, Organismal Injury and Abnormalities	Pancreatic cancer	miR-143-3p, miR-145-5p, miR-16-5p, miR-34a-5p	4	6.2E-03
Cancer, Organismal Injury and Abnormalities	Head and neck carcinoma	miR-143-3p, miR-16-5p, miR-26a-5p, miR-34a-5p	4	6.6E-03
Cancer, Organismal Injury and Abnormalities	Pelvic tumor	miR-143-3p, miR-145-5p, miR-16-5p, miR-187-3p, miR-26a-5p, miR-34a-5p	6	7.6E-03

Supplementary Table 8: Selected predicted target genes of miR-34a obtained using the indicated target prediction algorithms. Genes were filtered for their involvement in cAMP signaling.

	human				rat			mouse			
	Target Scan	miRANDA	DIANA tools	PITA	Target Scan	miRANDA	DIANA tools	Target Scan	miRANDA	DIANA tools	PITA
AIP						X					
AhR		X							X		
PDE1a									X		X
PDE1b		X							X		
PDE1c						X	X		X		
PDE2a								X	X		
PDE3a	X				X			X			
PDE4a		X		X							X
PDE4b	X	X	X	X				X			
PDE4c		X									
PDE4d					X			X			
PDE4dip									X		X
PDE5a		X			X	X		X	X		
PDE6g									X		
PDE6h								X			
PDE7a	X		X	X					X		
PDE7b	X	X	X			X			X		
PDE8a					X			X			
PDE8b									X		
PDE10a					X			X		X	
PDE11a			X	X	X						
PDE12								X			
GNAO1	X	X			X			X	X		X
GNAI1					X			X	X		
GNAI2	X	X			X	X	X	X	X		X
GNAI3		X			X			X			X
GNA12		X		X			X				
GNAL	X	X							X		
GNAQ	X		X		X			X	X	X	
GNAS	X	X		X					X		
GNAT1		X							X		
GNAT2											
GNAZ		X		X		X					

Supplementary Table 9: Candidate target genes of miR-34a predicted by at least one algorithm in each species.

	human				rat			mouse			
	Target Scan	miRANDA	DIANA tools	PITA	Target Scan	miRANDA	DIANA tools	Target Scan	miRANDA	DIANA tools	PITA
PDE3a	X				X			X			
PDE5a		X			X	X		X	X		
PDE7b	X	X	X			X			X		
GNAO1	X	X			X			X	X		X
GNAI2	X	X			X	X	X	X	X		X
GNAI3		X			X			X			X
GNAQ	X		X		X			X	X	X	